ELSEVIER

Biochemical Pharmacology 61 (2001) 573–578

Biochemical Pharmacology

Ultrastructural morphology and localisation of cisplatin-induced platinum–DNA adducts in a cisplatin-sensitive and -resistant human small cell lung cancer cell line using electron microscopy

Coby Meijer[a,*], Marja J.A. van Luyn[b], Edith F. Nienhuis[a], Nel Blom[c], Nanno H. Mulder[a], Elisabeth G.E. de Vries[a]

[a]*Department of Medical Oncology, P.O. Box 30.001, University Hospital Groningen, 9700RB Groningen, The Netherlands*
[b]*Department of Medical Biology: Tissue Engineering, P.O. Box 30.001, University Hospital Groningen, 9700RB Groningen, The Netherlands*
[c]*Department of Haematology, P.O. Box 30.001, University Hospital Groningen, 9700RB Groningen, The Netherlands*

Received 14 January 2000; accepted 9 August 2000

Abstract

Ultrastructural morphology (transmission electron microscopy) and localisation of cisplatin-induced platinum (Pt)–DNA adducts (immunoelectron microscopy) were analysed in the human small cell lung cancer cell line GLC_4 and its 40-fold *in vitro* acquired cisplatin-resistant subline GLC_4-CDDP, which is characterised by, among other things, a decreased DNA platination. Immunolabelling of Pt–DNA adducts was performed with the polyclonal antibody GPt, known to detect the main Pt-containing intrastrand and interstrand DNA adducts. Morphological analysis of GLC_4 and GLC_4-CDDP at the ultrastructural level showed cells with a high nucleus/cytoplasm ratio with the majority of nuclei containing one or more nucleoli. GLC_4-CDDP showed, in contrast to GLC_4, an extensive Golgi apparatus and an increased number of mitochondria. DNA platination was detectable in both GLC_4 and GLC_4-CDDP. Immunoelectron microscopy showed Pt–DNA adducts primarily in the nucleus, preferentially at loci with high-density chromatin (e.g. heterochromatin, pars granulosa around nucleoli, condensed DNA in proliferating and apoptotic cells), and in mitochondria. The level of detectable Pt–DNA adducts was cell cycle status-dependent. In both cell lines, Pt–DNA adduct levels increased from non-dividing interphase cells to dividing cells and were highest in cells undergoing apoptosis. Overall localisation of Pt–DNA adducts was comparable in GLC_4 and GLC_4-CDDP cells.

Keywords: Ultrastructural morphology; Electron microscopy; Ultrastructural localisation; Cisplatin; Pt–DNA adducts; Immunoelectron microscopy

1. Introduction

Cisplatin is one of the most important chemotherapeutic drugs in clinical practice [1]. Although the mode of action of cisplatin has been under intensive study since its discovery more than 30 years ago, the exact mechanism of action of this drug has yet to be defined [2,3]. Many studies have focused on the level of DNA platination as a measure of cisplatin-induced damage. Four major Pt–DNA adducts were detected and extensively studied [2–5]. Little is known about the precise localisation or distribution of the Pt–DNA adducts, i.e. either within the nucleus or outside it in the cytoplasm in e.g. the mitochondria of cells, or about the appearance of differences in the distribution of Pt–DNA adducts between different (e.g. sensitive or resistant) cells.

The present study evaluated ultrastructural cellular morphology and localisation of cisplatin-induced Pt–DNA adducts in the human small cell lung cancer cell line GLC_4 and its *in vitro* acquired cisplatin-resistant subline GLC_4-CDDP with transmission electron and immunoelectron microscopy, respectively. Immunolabelling of Pt–DNA adducts was performed with the polyclonal antibody GPt, known to detect the main Pt-containing intrastrand and interstrand DNA adducts [6].

* Corresponding author. Tel.: +31-50-361-3594; fax: +31-50-361-4862.
E-mail address: j.meijer@int.azg.nl (J. Meijer).
Abbreviation: Pt, platinum.

0006-2952/01/$ – see front matter
PII: S0006-2952(00)00584-0

2. Materials and methods

2.1. Chemicals

RPMI-1640 medium and foetal bovine serum were purchased from Life Technologies. Cisplatin was obtained from Bristol Myers. Paraformaldehyde and glutaraldehyde were from Polysciences Inc., Epon 812 was from Serva, unicryl from SanverTech, and methylcellulose from Fluka. Nickel grids were obtained from Stork, and formvar 15/95E from Balzers Union. BSA was provided by the CLB and gold-conjugated (5 nm) goat anti-rabbit immunoglobulin from British Biocell International.

2.2. Cell lines

The human small cell lung cancer cell line GLC_4 and its 40-fold *in vitro* acquired cisplatin resistant GLC_4-CDDP were used. Resistance to cisplatin in GLC_4-CDDP coincided with an unchanged cellular Pt level, an increased glutathione level, decreased DNA platination, and increased DNA repair [7–9]. Both cell lines were routinely cultured in RPMI-1640 medium supplemented with 10% heat-inactivated foetal bovine serum, at 37°, in a humidified atmosphere with 5% CO_2. To maintain stable resistance, GLC_4-CDDP was incubated monthly with 75 μg/mL of cisplatin for 1 hr.

2.3. Morphology analysis by transmission electron microscopy

GLC_4 and GLC_4-CDDP cells ($\pm$ 5 $\times$ 10^6) were washed twice with PBS (0.14 M NaCl, 2.7 mM KCl, 6.4 mM $Na_2HPO_4 \cdot 2H_2O$, and 1.5 mM KH_2PO_4, pH 7.4) at 4°, pelleted, and prefixed with 2% glutaraldehyde in 0.1 M phosphate buffer for at least 2 hr at 4°. Cell blocks ($\pm$ 3 $\times$ 3 mm) were prepared and rinsed thoroughly in phosphate buffer, postfixed in 1% OsO_4 for 1 hr, dehydrated through a graded series of ethanols, and embedded in Epon 812. Morphology of cells was analysed in ultrathin sections (80 nm) after staining with uranyl acetate and lead citrate in a Philips 201 transmission electron microscope.

2.4. Localisation of Pt–DNA adducts by immunoelectron microscopy

GLC_4 and GLC_4-CDDP cells ($\pm$ 10 $\times$ 10^6) were incubated for 4 hr with 0, 16.5, 82.5, and 333 μM cisplatin, subsequently washed twice with PBS at 4°, and pelleted. Pellets were fixed with 4% paraformaldehyde for 2 hr and, after dehydration through a graded series of ethanols, were infiltrated overnight with unicryl, all at 4°. Polymerisation was performed under UV light (approximately 2 days at 4°). Before cutting, specimens were placed at 60° for at least 1 hr, which turned out to be essential for an optimal immunodetection of Pt–DNA adducts. Ultrathin sections (100 nm) were collected on formvar-coated nickel grids and air-dried.

2.5. Immunolabelling of Pt–DNA adducts

GPt, a polyclonal antibody against platinated DNA, known to detect the main Pt-intrastrand cross-links (i.e. the Pt–GG adducts) and interstrand cross-links, was used for immunohistochemical detection of Pt–DNA adducts [6]. Upon staining, sections were placed face down on PBS before incubation with 1 % BSA in PBS (20 min) to block non-specific antibody binding followed by an overnight treatment with GPt (1:200) at room temperature. After washing with PBS, the presence of Pt–DNA adducts was detected by incubation with 5-nm gold particles coated with goat anti-rabbit immunoglobulin for 60 min. After washing with PBS, sections were stained, covered with a methylcellulose uranylacetate mixture (9:1) for 10 min at 4°, and air-dried. Evaluation was performed with the Philips 201 transmission electron microscope. Staining without the first antibody (GPt) served as staining control, while staining with GPt in non-drug-treated cells was used as background staining control for each cell line. Quantitative analysis was performed by counting the gold labels per cm^2 of area of interest on photographs of at least 3 individual cells. Analysis was performed for both cell lines at each tested cisplatin concentration in non-dividing interphase cells, dividing cells, and cells undergoing apoptosis.

3. Results

Morphological analysis of GLC_4 and GLC_4-CDDP at the ultrastructural level showed cells with a high nucleus: cytoplasm ratio (Fig. 1). The majority of the nuclei contained one or more large nucleoli. GLC_4-CDDP showed, in contrast to GLC_4, an extensive Golgi apparatus and an increased number of mitochondria (Fig. 1b). No morphological or quantitative differences in mitotic or apoptotic figures were observed.

DNA platination was detected by immunoelectron microscopy in both GLC_4 and GLC_4-CDDP. Localisation of the Pt–DNA adducts was primarily in the nucleus, preferentially at loci with high-density chromatin (heterochromatin, pars granulosa around nucleoli, condensed DNA in proliferating and apoptotic cells), but also in mitochondria. Staining controls were negative whereas, as expected, some background labelling could be observed in both cell lines. The amount of detectable Pt–DNA adducts in non-dividing interphase cells of both cell lines was very low and comparable to the levels observed in the background controls ($<$ 0.1 gold labels per cm^2 for both cell lines at all tested cisplatin concentrations). Fig. 2 shows the quantitative analysis of the amount of Pt–DNA adducts at the ultrastructural level in dividing and apoptotic GLC_4 and GLC_4-CDDP cells after 4-hr incubation with cisplatin. GLC_4 showed a

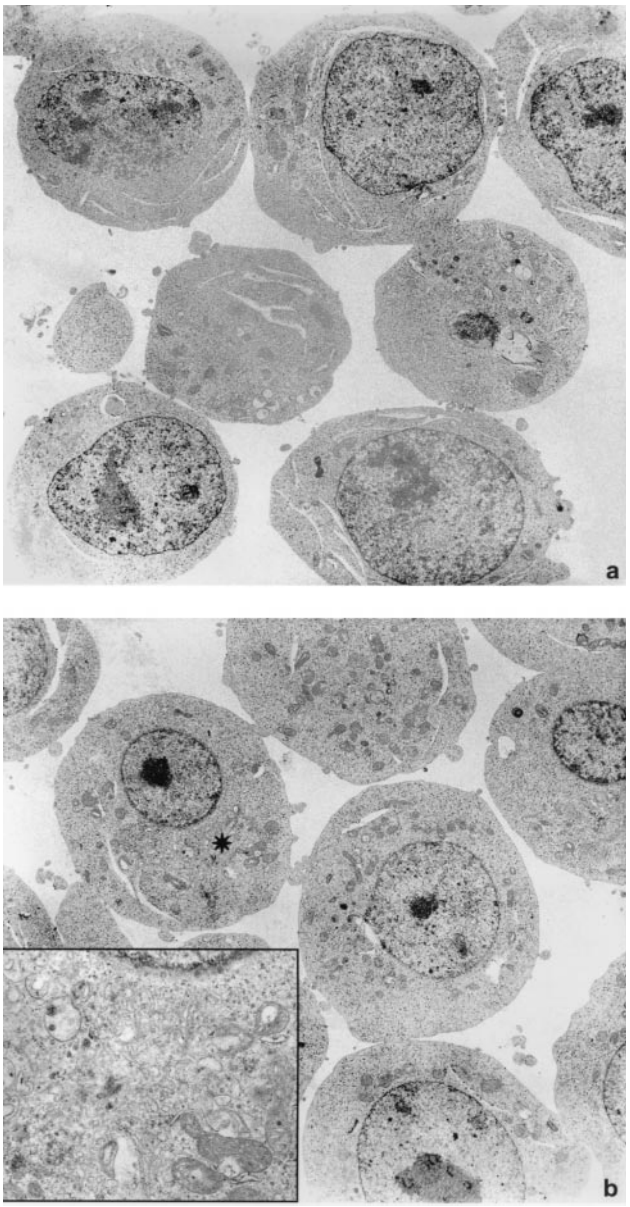

Fig. 1. Electron micrographs of GLC_4 (a) and GLC_4-CDDP (b) at magnifications 4700×: cells show a high nucleus:cytoplasm ratio with one or more large nucleoli in the majority of the nuclei. GLC_4-CDDP showed, in contrast to GLC_4, an extensive Golgi apparatus and an increased number of mitochondria (b; the asterisk is pointed out in detail in the inset).

dose-dependent increase in immunolabelling in both dividing and apopotic cells (Fig. 2, A and C). Immunolabelling of apoptotic cells was 10- to 20-fold higher than in dividing cells. Immunolabelling of the dividing GLC_4-CDDP cells was comparable to GLC_4 (Fig. 2B). GLC_4-CDDP cells undergoing apoptosis showed a low level of immunolabelling at the 16.5- and 82.5-μM cisplatin concentrations, whereas at the highest concentration (333 μM) a high level of immunolabelling could be observed (Fig. 2D). The level of detectable Pt–DNA adducts was cell cycle status-dependent. In both cell lines, Pt–DNA adduct levels increased from non-dividing interphase cells to dividing cells and were highest in cells undergoing apoptosis (Fig. 3, A–C). No direct effect of cisplatin treatment on cell viability (trypan blue dye exclusion) or cell cycle distribution was observed. Both GLC_4 and GLC_4-CDDP showed a variable level of detectable Pt–DNA adducts in their mitochondria (ranging from none to 5 gold labels per mitochondrion; median: 2–3 gold labels per mitochondrion (Fig. 3D)). No difference in labelling of mitochondria was observed between the cell lines. Overall, localisation of Pt–DNA adducts was comparable in the two cell lines.

4. Discussion

The present study evaluated ultrastructural morphology and ultrastructural localisation of Pt–DNA adducts in the human small cell lung cancer cell line GLC_4 and its 40-fold *in vitro* acquired cisplatin-resistant subline GLC_4-CDDP. Resistance to cisplatin in GLC_4-CDDP coincided with an unchanged cellular Pt level, an increased glutathione level, decreased DNA platination, and increased DNA repair [7–9].

Morphological analysis of GLC_4 and GLC_4-CDDP showed cells with a high nucleus/cytoplasm ratio with the majority of nuclei containing one or more nucleoli. GLC_4-CDDP showed, in contrast to GLC_4, an extensive Golgi apparatus and an increased number of mitochondria. Little is known about the impact of cisplatin on tumour cell mitochondria. Andrews and Albright [10] described changes in both mitochondrial membrane potential and morphology in a cisplatin-resistant human ovarian cancer cell line (C13*). Mitochondria showed smaller, stained denser, and displayed a higher crystal density, although no increase in the quantity of mitochondria was reported. Similar morphology differences of mitochondria were reported in photodynamic therapy-resistant cells, which turned out to be cross-resistant to cisplatin [11,12]. Moreover, the cisplatin-resistant C13* cells appeared to be cross-resistant to photodynamic therapy [11]. Cisplatin-resistant cells may directly benefit from quantitatively and/or functionally more active mitochondria (increased membrane potential), as these phenomena are linked to an increase in oxidative phosphorylation and thereby an increase in energy production/metabolism (e.g. suitable for increased DNA repair). Indirectly, mitochondria can be involved in sensitivity to cisplatin by modulation of signal transduction pathways, leading to cell death [13].

Detection of Pt–DNA adducts by immunoelectron microscopy with the GPt antibody was feasible in both cell lines. In cryosections, however, we were not able to detect Pt–DNA adducts. The use of unicryl combined with incubation at a high temperature of 60° after polymerisation under UV light at 4° turned out to be essential for immunodetection of Pt–DNA adducts with the GPt antibody. Localisation of the Pt–DNA adducts was, as expected, primarily found in the nucleus, but especially at loci with

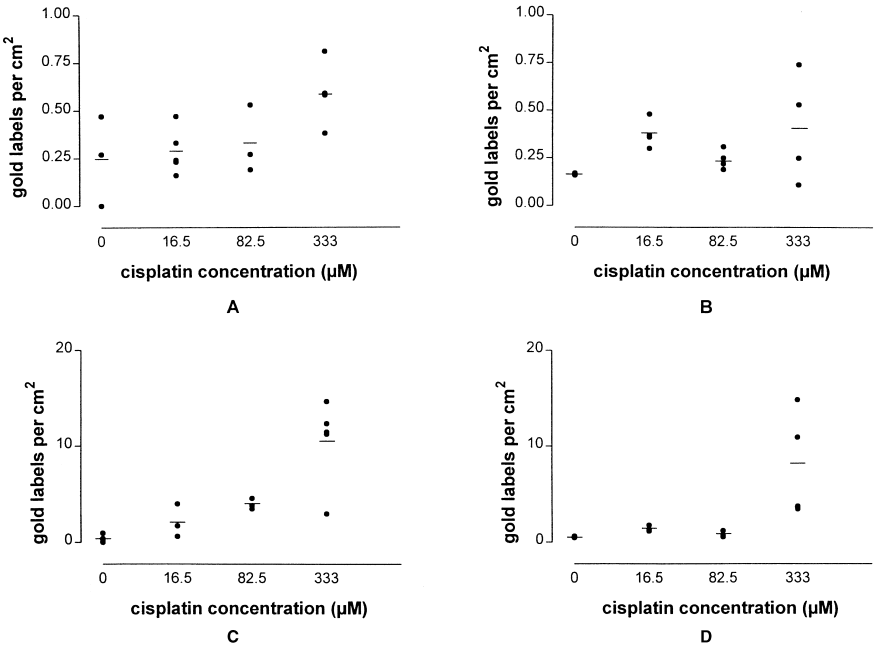

Fig. 2. Quantitative analysis of the amounts of Pt–DNA adducts at the ultrastructural level in GLC_4 and GLC_4-CDDP after 4-hr incubation with cisplatin. Each point represents an individual cell (the mean is indicated by the dash). (A) dividing GLC_4 cells; (B) dividing GLC_4-CDDP cells; (C) apoptotic GLC_4 cells; (D) apoptotic GLC_4-CDDP cells.

high-density chromatin: heterochromatin and condensed DNA in proliferating and apoptotic cells. Heterochromatin contains about 10% of the genome and is known to be transcriptionally inactive. Therefore, euchromatin, the more diffuse transcriptionally active part of chromatin, seems to be the more logical target for DNA-directed drugs [14,15]. To some extent, the high levels of Pt–DNA adducts in heterochromatin may reflect the higher density of DNA in heterochromatin compared to euchromatin. Accessibility may also play a role. However, the observed cisplatin dose–response relation within the same areas of interest underlines a variation in adduct levels rather than a variation in the ability to access and recognise adducts. We attempted to combine the sensitivity of our antibody with the great resolving power of electron microscopy to obtain an impression of the localisation of Pt–DNA adducts in both cell lines. Especially in the case of immunoelectron microscopy, detection at the ultrastructural level does not necessarily equate with high levels of sensitivity. Fixation demands for electron microscopy together with the use of ultrathin sections, the evaluation of small numbers of cells, and epitope diversity limit a quantitative application. Indeed, in our case much higher cisplatin incubation concentrations compared to our sensitive immunocytochemical technique were needed to detect Pt–DNA adducts. Within the limitations mentioned above, a quantitative analysis was performed for both cell lines at each cisplatin concentration. The level of detectable Pt–DNA adducts was cell cycle status-dependent. In both cell lines, Pt–DNA adduct levels increased from non-dividing interphase cells to dividing cells and were highest in cells undergoing apoptosis. No data on Pt–DNA adduct levels in cells undergoing apoptosis are available. It is of interest that apoptotic cells, and especially cisplatin-resistant GLC_4-CDDP cells in apoptosis, show high levels of Pt–DNA adducts. Pt–DNA adducts were also clearly detectable in mitochondria. Mitochondrial DNA is a very well-conserved sequence of approximately 16,500 base pairs of double-stranded circular DNA and may be an easy target for DNA-damaging agents because it lacks histones to protect the DNA. Although GLC_4-CDDP showed an increased number of mitochondria compared to GLC_4, no obvious difference in the labelling index of the mitochondria was observed between GLC_4 and GLC_4-CDDP. Until now, only Olivero *et al*. [16] had shown localisation of Pt–DNA adducts using immunoelectron microscopy. Surprisingly, in their study gold particles associated with Pt–DNA adducts were found to a similar extent in both the nucleus and cytoplasm of cisplatin-treated Chinese hamster ovary (CHO) cells, thereby questioning the epitope recognition of the antibody used against cisplatin–DNA adducts under their described experimental conditions. They reported preferential binding of cisplatin to mitochondrial DNA, which was confirmed in isolated mitochondrial and genomic DNA by use of a competitive immunoassay. Both higher initial binding and the lack of removal of Pt–DNA adducts appeared to contribute to the preferential binding of cisplatin to mitochondrial DNA in CHO cells [17]. Murata *et al*. also showed more efficient binding of cisplatin to mitochondrial DNA as compared to genomic DNA, which coincided with the suppression of ATP generation in human malignant melanoma cells [18]. Overall, in our study local-

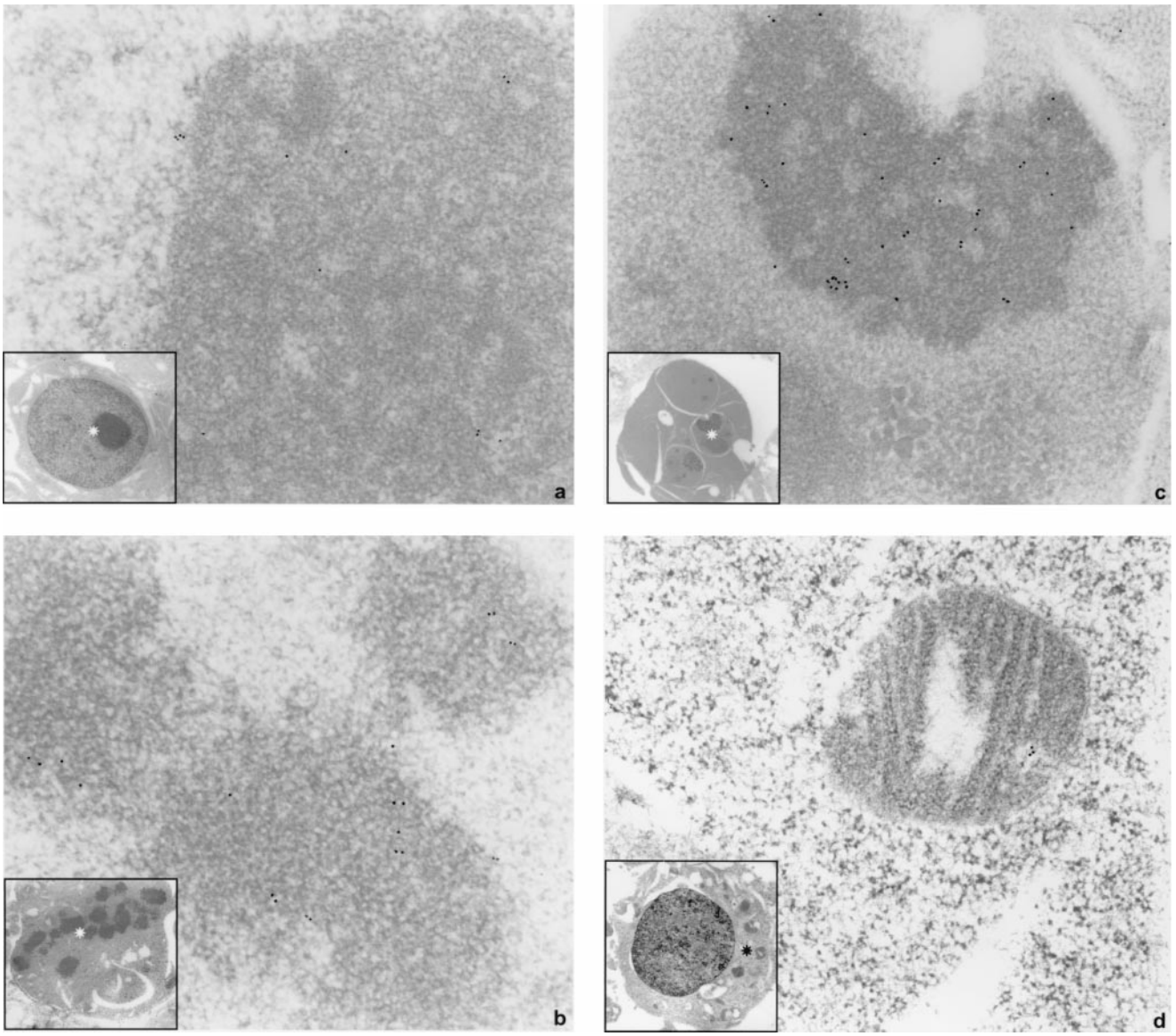

Fig. 3. Electron micrographs at magnifications 67,000×: ultrastructural localisation of cisplatin-induced Pt–DNA adducts (5 nm gold particles) in representative GLC_4 cells incubated for 4 hr with 16.5 μM cisplatin. (a): detection of Pt–DNA adducts in a part of a nucleolus of a non-dividing interphase GLC_4 cell; inset: survey of the GLC_4 cell (magnification 10,750×); (b): increased levels of Pt–DNA adducts in condensed DNA of a dividing GLC_4 cell; inset: survey of the GLC_4 cell (magnification 10,750×); (c): highest level of Pt–DNA adducts in an apoptotic body of an apoptotic GLC_4 cell; inset: survey of the GLC_4 cell (magnification 15,500×); (d): detection of Pt–DNA adducts in a mitochondrion of a non-dividing GLC_4 cell; inset: survey of the GLC_4 cell (magnification 10,750×).

isation of Pt–DNA adducts was comparable in GLC_4 and GLC_4-CDDP cells.

In summary, cisplatin-resistant GLC_4-CDDP cells showed an extensive Golgi apparatus and an increased number of mitochondria compared to the parent GLC_4. DNA platination was detected at the ultrastructural level in both GLC_4 and GLC_4-CDDP, primarily in the nucleus but also in the mitochondria. The level of detectable Pt–DNA adducts was cell cycle status-dependent, increasing from non-dividing interphase cells to dividing cells and highest in cells undergoing apoptosis. Ultrastructural localisation of Pt–DNA adducts did not differ in cisplatin-sensitive and-resistant cells.

Acknowledgement

The authors acknowledge the assistance of B.F.A. Hellinga (photography; Department of Cell Biology and Electron Microscopy, University of Groningen, the Netherlands).

References

[1] Loehrer PJ, Einhorn LH. Cisplatin. Ann Intern Med 1984;100:704–13.
[2] Andrews PA, Howell SB. Cellular pharmacology of cisplatin: perspectives on mechanisms of acquired resistance. Cancer Cells 1990; 2:35–43.

[3] Timmer-Bosscha H, Mulder NH, de Vries EG. Modulation of *cis*-diamminedichloroplatinum(II) resistance: a review. Br J Cancer 1992;66:227–38.
[4] Lippard SJ. New chemistry of an old molecule: *cis*-[$Pt(NH_3)_2Cl_2$]. Science 1982;218:1075–82.
[5] Fichtinger-Schepman AM, van der Veer JL, den Hartog JH, Lohman PH, Reedijk J. Adducts of the antitumor drug *cis*-diamminedichloroplatinum(II) with DNA: formation, identification, and quantitation. Biochemistry 1985;24:707–13.
[6] Meijer C, de Vries EG, Dam WA, Wilkinson MH, Hollema H, Hoekstra HJ, Mulder NH. Immunocytochemical analysis of cisplatin-induced platinum–DNA adducts with double-fluorescence video microscopy. Br J Cancer 1997;76:290–8.
[7] Hospers GA, Mulder NH, de Jong B, de Leij L, Uges DR, Fichtinger-Schepman AM, Scheper RJ, de Vries EG. Characterization of a human small cell lung carcinoma cell line with acquired cisplatin resistance *in vitro*. Cancer Res 1988;48:6803–7.
[8] Hospers GA, Meijer C, de Leij L, Uges DR, Mulder NH, de Vries EG. A study of human small cell lung carcinoma (hSCLC) cell lines with different sensitivities to detect relevant mechanisms of cisplatin (CDDP) resistance. Int J Cancer 1990;46:138–44.
[9] Meijer C, Mulder NH, Hospers GA, Uges DR, de Vries EG. The role of glutathione in resistance to cisplatin in a human small cell lung cancer cell line. Br J Cancer 1990;62:72–77.
[10] Andrews PA, Albright KD. Mitochondrial defects in *cis*-diamminedichloroplatinum(II)-resistant human ovarian carcinoma cells. Cancer Res 1992;52:1895–1901.
[11] Sharkey SM, Wilson BC, Moorehead R, Singh G. Mitochondrial alterations in photodynamic therapy-resistant cells. Cancer Res 1993;53:4994–9.
[12] Moorehead RA, Armstrong SG, Wilson BC, Singh G. Cross-resistance to cisplatin in cells resistant to photofrin-mediated photodynamic therapy. Cancer Res 1994;54:2556–9.
[13] Decaudin D, Geley S, Hirsch T, Castedo M, Marchetti P, Macho A, Kofler R, Kroemer G. Bcl-2 and Bcl-X_L antagonize the mitochondrial dysfunction preceding nuclear apoptosis induced by chemotherapeutic agents. Cancer Res 1997;57:62–7.
[14] Johnson S. The cell nucleus. In: Alberts B, Bray D, Lewis J, Raff M, Roberts K, Watson JD, editors. Molecular Biology of the Cell. New York & London: Garland Publishing Inc., 1994. p. 336–96.
[15] Bubley GJ, Xu J, Kupiec N, Sanders D, Foss F, O'Brien M, Emi Y, Teicher BA, Patierno SR. Effect of DNA conformation on cisplatin adduct formation. Biochem Pharmacol 1996;51:717–21.
[16] Olivero OA, Semino C, Kassim A, Lopez-Larraza DM, Poirier MC. Preferential binding of cisplatin to mitochondrial DNA of Chinese hamster ovary cells. Mutat Res 1995;346:221–30.
[17] Olivero OA, Chang PK, Lopez-Larraza DM, Semino-Mora MC, Poirier MC. Preferential formation and decreased removal of cisplatin–DNA adducts in Chinese hamster ovary cell mitochondrial DNA as compared to nuclear DNA. Mutat Res 1997;391:79–86.
[18] Murata T, Hibasami H, Maekawa S, Tagawa T, Nakashima K. Preferential binding of cisplatin to mitochondrial DNA and suppression of ATP generation in human malignant melanoma cells. Biochem Int 1990;20:949–55.